약학석사 학위논문

Structural Studies on SAV0324 from *Staphylococcus aureus* by X-ray Crystallography

X-선 결정학에 의한 황색포도상구균 유래 SAV0324 단백질의 구조 연구

2017년 8월

서울대학교 대학원

약학과 물리약학전공

구 지 성

Structural Studies on SAV0324 from *Staphylococcus aureus* by X-ray Crystallography

X-선 결정학에 의한 황색포도상구균 유래
SAV0324 단백질의 구조 연구

지도교수 이 봉 진

이 논문을 약학석사 학위논문으로 제출함
2017년 6월

서울대학교 대학원
약학과 물리약학전공
구 지 성

구지성의 석사 학위논문을 인준함
2017년 6월

위 원 장 변 영 로 (인)

부위원장 오 유 경 (인)

위 원 이 봉 진 (인)

Abstract

Structural Studies on SAV0324 from *Staphylococcus aureus* by X-ray Crystallography

Ji Sung Koo
College of Pharmacy, Seoul National University

Staphylococcus aureus is a gram positive bacteria which produces enzymes, toxins, and small RNAs that are often harmful to the body. About 20-30% of the human population are carriers of the bacteria and the bacteria is responsible for causing many diseases and casualties worldwide.

SAV0324 is a glycine cleavage system H-like protein (GcvH-L) which acts as a carrier for lipoyl moiety. SAV0324 undergoes lipoylation by SAV0327 protein and subsequently undergoes ADP-ribosylation process. Without ADP-ribosylation, the virulence of *Staphylococcus aureus* bacteria decreases and therefore, inhibition of lipoylation would be crucial.

Using Structure Based Drug Design (SBDD) as a background knowledge, the structure of SAV0324 protein was determined at 1.88Å. Specifically, SAV0324 conserved five alpha-helices and nine beta-strands in its structure and the site of lipoylation in SAV0324 was already determined to be E53 (53^{rd} glutamate) and K56 (56^{th}

lysine) residues by other researchers. Furthermore, crystallization of SAV0327 protein was successful. Through binding test between SAV0324 and SAV0327, the results showed the two proteins did not have direct binding interaction in the absence of lipoic acid. Thus, in addition to SAV0324's structural information, determination of SAV0327 protein structure and its active site would be of great significance. Knowing both SAV0324 and SAV0327 thoroughly would be critical in controlling and understanding bacterial virulence of *Staphylococcus aureus*.

Keywords : Structure Based Drug Design (SBDD), *Staphylococcus aureus*, X-ray crystallography, SAV0324, lipoylation, virulence

Student Number : 2015-23174

Contents

List of Tables

List of Figures

Abbreviations

3D	Three-dimensional
CD	Circular Dichroism
IMAC	Immobilized Metal Affinity Chromatography
SEC	Size Exclusion Chromatography
EDTA	Ethylenediaminetetraacetic acid
IPTG	Isopropyl-β-D-thiogalacopyranoside
LA	Lipoic Acid
ATP	Adenosine Triphosphate
LB	Luria-Bertani
OD	Optical Density
SDS-PAGE	Sodium Dodecyl Sulfate - PolyAcrylamide Gel Electrophoresis
PCR	Polymerase Chain Reaction
pET	Plasmid for Expression using T7 promoter

I. General Introduction

1.1 *Staphylococcus aureus*

Staphylococcus aureus is a round-shaped, gram-positive bacteria usually located in the nose, respiratory tract, and on the skin (Masalha et al., 2001). The bacteria has the ability to colonize individuals asymptomatically and about 20-30% of the human population are carriers of the bacteria (Chambers and DeLeo, 2009). The bacteria's asymptomatic colonization is far more common than infection (Chambers, 2001); however, upon infection by pathogenic strains, the bacteria produces enzymes (Cheesbrough, 1991), toxins (Dinges, Orwin, and Schlievert, 2000), and small RNAs (Bohn et al., 2010) which are harmful to the body. In addition, *Staphylococcus aureus* bacteria is passed on from one to another through direct contact with an infected individual or with a contaminated surface (Himaratsu, Cui, Kuroda, and Ito, 2001).

One major problem associated with *Staphylococcus aureus* is its heavy resistance to antibiotics (Chambers and DeLeo, 2009). The bacteria developed heavy resistance strains including MRSA and (Grundmann, Aires-de-Sousa, Boyce, and Tiemersma, 2006) and VRSA strains (Weigel et al., 2003). There are no approved vaccines against *Staphylococcus aureus* and to make matters worse, the bacteria is known to cause many conditions such as hospital-acquired bacteremia, toxic shock syndrome, surgical wound infection and much more (Archer, 1998).

1.2 SAV0324

The target protein, SAV0324 is a glycine cleavage system H-like protein and also a carrier for lipoyl moiety. The SAV0324 protein, along with lipoic acid and adenosine triphosphate, undergoes lipoylation by SAV0327 protein (Figure 1). The lipoylated form of SAV0324 subsequently undergoes ADP-ribosylation and reverse ADP-ribosylation by SAV0326 and SAV0325 proteins respectively (Rack et al., 2015). This overall cycle is known to be very crucial to *Staphylococcus aureus* because ADP-ribosylation cycle is known to modulate virulence of the bacteria (Deng and Barbieri, 2008).

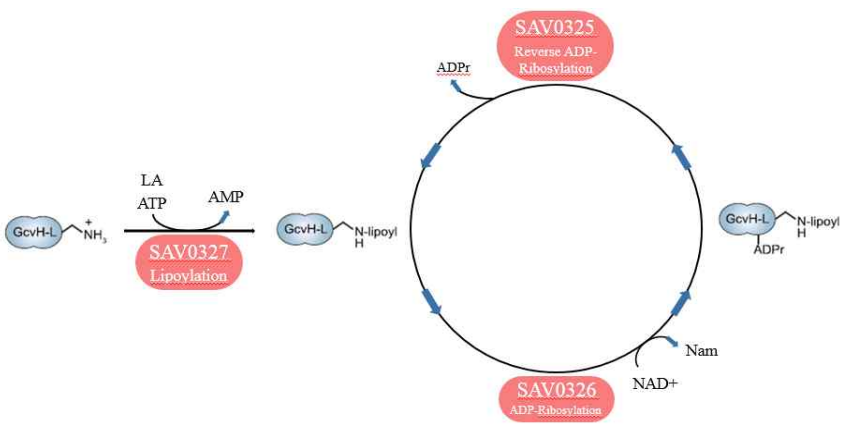

Figure 1. ADP-ribosylation cycle in *Staphylococcus aureus*

SAV0324 consists of 110 amino acid residues and its molecular weight is about 12.42 kDa. Theoretical pI value is 4.12 and its extinction coefficient is 15470 $M^{-1}cm^{-1}$. The instability index (II) of SAV0324 protein is computed to be 36.42, which classifies the protein as stable.

1.3 Structure Based Drug Design (SBDD)

Structure Based Drug Design (SBDD) is an effective and a rational drug design/discovery method which utilizes the three-dimensional structure of the protein as a template for designing novel drug candidates. Initially, the purified target protein is used to determine the three-dimensional structure of the protein usually accomplished using NMR spectroscopy or X-ray crystallography (Figure 2).

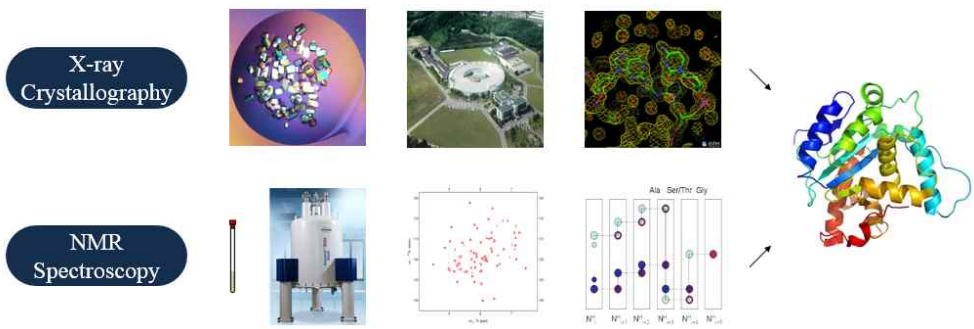

Figure 2. Structure determination through NMR-spectroscopy / X-ray Crystallography

Upon protein structure and active site determination, many drug candidates from various chemical libraries can be screened for viability and effectivity. The main goal is to optimize and generate lead compounds capable of inhibiting and inactivating the protein of interest and ultimately designing a novel drug compound. Like a lock-and-key model, only specific drug molecule will fit into the active site of the protein. Only under specific conditions, the lock will open, leading to discovery of a new drug molecule (Figure 3).

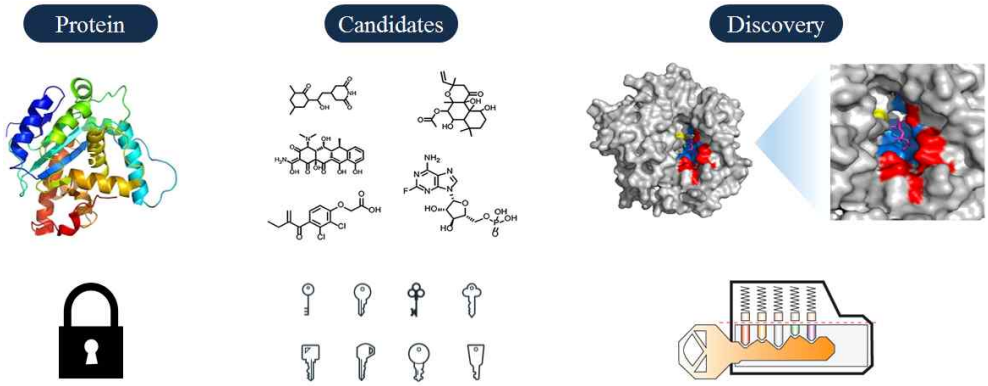

Figure 3. Analogy between drug and lock-and-key model

Compared to old trial and error traditional drug design, structure based drug design has many advantages. Some advantages include low toxicity, higher efficiency, high reasonability, low cost, shorter development time and higher clinical entry rate.

An example of a drug developed through SBDD is Gleevec. The drug binds in the active site of the CML enzyme, restricting two ATP molecules from interacting with each other. Gleevec inhibits the function of CML enzyme, ultimately resulting in the suppression of myeloid leukemia. Other examples of drugs developed through structure based drug design include Tamiflu, Viagra, Reyataz, Aluviran, Tarceva, and much more.

II. Purpose of Study

The main purpose of this study is to determine the structure of SAV0324 protein from *Staphylococcus aureus* through X-ray crystallography. SAV0324 protein is known to be a carrier for lipoyl moiety, therefore inhibition of SAV0324's active site would inhibit lipoylation. Inhibition of lipoylation would subsequently inhibit ADP-ribosylation, ultimately resulting in decreased virulence of *Staphylococcus aureus*.

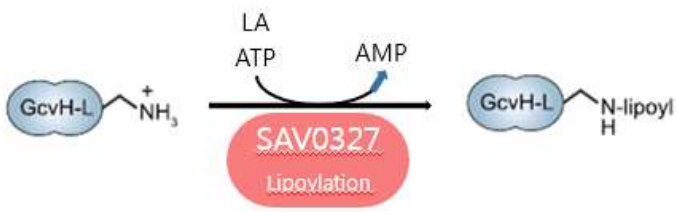

Figure 4. SAV0324 lipoylation by SAV0327

Another goal of this study is to initiate structure determination process of SAV0327 protein. Determination of SAV0327 protein and its active would be critical in understanding lipoylation and ultimately controlling bacterial virulence of *Staphylococcus aureus*.

Ultimately, upon structure determination, screening of compounds from various chemical library can be conducted. Through lead optimization, drug molecule candidates with high efficiency and less toxicity will become available. Therefore, discovery of a new drug molecule capable of inhibiting lipoylation and decreasing bacterial virulence is theoretically possible.

III. Materials and Methods

2.1 Materials

2.1.1 Reagents

Staphylococcus aureus genomic DNA (strain Mu50 / ATCC700699) was used for experimental procedures. PCR premix kits were purchased from Intron Biotechnology and restriction enzymes (NdeI & XhoI) along with Cutsmart buffer were purchased from New England Biolabs (NEB). Sequencing was performed by Cosmogenetech and NICEM. Isopropyl β-D-1-thiogalactopyranoside (IPTG) was purchased from Calbiochem and Ampicillin was purchased from Biosesang. Tris-HCl, sodium chloride (NaCl) and hydrochloric acid (HCl) was purchased from Dongin Biotechnology. Lastly, crystallization kits were purchased from Molecular Dimensions and Hampton Research.

2.1.2 Apparatus

Polymerase Chain Reaction (PCR) was carried out by Bio-Rad T100 Thermal Cycler and Cole-Parmer Ultrasonic Processor was used for cell lysis. Concentration of protein was performed by centrifugal filter units from Merck Millipore. Immobilized metal affinity chromatography was performed using HiTrap Chelating HP and size exclusion chromatography was performed using HiLoad 16/600 Superdex 200pg. Circular Dichroism (CD) spectroscopy measurements

were made using Chirascan plus from Applied Photophysics and MALDI-TOF measurements were made using Voyager-DE from Applied Biosystems. X-ray diffraction data were collected at PAL (Pohang, South Korea) using an ADSC quantum 315r CCD detector on 5C-SBII bealimline at 100K. The raw data were processed using HKL2000 program and the structure of SAV0324 was solved by molecular replacement method using CCP4 program.

2.2 Methods

2.2.1 Cloning

Polymerase Chain Reaction (PCR) is a technique used to amplify a DNA segment of interest into thousands or millions of copies of the same particular DNA sequence (Saiki et al., 1988).

The gene encoding SAV0324 protein from *Staphylococcus aureus* was amplified by PCR using *Staphylococcus aureus* genomic DNA (strain Mu50 / ATCC700699) as a template. The forward primer was : 5'-CATATGAAAAAGTTAGCCAATTATTTATGG - 3' and the reverse primer was : 5'-CTCGAGTTAAGCCTCCGGTAATGCTAG-3' where the underlined sequences represent NdeI and XhoI restriction sites respectively. The amplified insert and pET21(+) vector was processed with restriction enzymes (NdeI and XhoI) and Cutsmart buffer at 37°C for 3 hours and were ligated together using ligation mix at 20°C for 1 hour. The ligated product was transformed with DH5α competent cell and was incubated on ampicillin plate overnight at 37°C. The overnight grown colonies were grown were sent for

sequencing. Sequencing result was successful and SAV0324-pET21a plasmid was further transformed with six competent cells : BL21DE3, BL21DE3Codon+, RosettaDE3, Rosetta2pLysS, C41DE3, and C43DE3.

The gene encoding SAV0327 protein from *Staphylococcus aureus* was also amplified using PCR. Following the same general procedures, SAV0327 was successfully cloned into pET21a(+) vector and was further transformed with same six competent cells isolated from *Escherichia coli* : BL21DE3, BL21DE3Codon+, RosettaDE3, Rosetta2pLysS, C41DE3, and C43DE3.

2.2.2 Overexpression Test

Overexpression of target protein is performed to obtain maximum amount of protein. Upon isopropyl β-D-1-thiogalactopyranoside (IPTG) induction, *lac* operon transcription is triggered, allowing overexpression of target protein (Marbach and Bettenbrock, 2012).

All six competent cells containing SAV0324-pET21a plasmid were cultivated overnight in Luria-Bertani (LB) medium containing ampicillin. The cultured cells were inoculated into new LB medium (200mL) and were incubated at 37°C-180rpm until optical density (O.D.) at 600nm reached 0.5. Sample was taken before IPTG induction. The cells were cooled at 4°C for around 15 minutes were induced by adding IPTG (0.25mM) into medium. The cells were incubated at 15°C-150rpm for 20 hours and sample was taken after 20 hours, corresponding to sample after IPTG induction. The cells were harvested using a centrifuge at 6,000rpm at 4°C for 10 minutes and were stored @-80°C. The samples were boiled at 95-100°C for

around 10 minutes and SDS-PAGE was performed using samples before and after IPTG induction.

Same protocol was conducted for SAV0327 proteins.

2.2.3 Solubility Test

Solubility test is performed to test if the proteins fall into either an insoluble inclusion body fraction or soluble protein fraction. The protein must be in its soluble fraction for further experiments.

SAV0324's harvested cells, in its pellet form, were suspended in Tris-HCl lysis buffer (20mM Tris, 500mM NaCl, pH 7.9) along with 10% of 50% v/v glycerol. The cells were placed in a steel cup and were suspended in ice. Sample was taken before sonication. Further, the cells were disrupted by ultrasonication process and sample was taken after sonication. The sample after sonication was centrifuged at 18,000rpm for 5 minutes and the pellet and supernatant was named P and S respectively. SDS-PAGE was performed using samples before sonication and after sonication (P and S). The lysate was centrifuged at 18,000rpm, 4°C for 60 minutes and the resulting supernatant was filtered using 0.45μm syringe filter.

Same process was conducted for SAV0327 proteins.

2.2.4 Affinity Chromatography (IMAC)

Affinity chromatography is a method which utilizes high specific interaction between molecules to separate a specific molecule from the

rest. Generally, the desired molecule will stay bound to the column while the undesired material will elute first (Ninfa, Ballou, and Benore, 2009).

Prior to loading filtered protein onto His-tag affinity column, the HiTrap Chelating HP column was washed in the following order : EDTA, FDW, Ni2+, and A buffer (20mM Tris, 500mM NaCl, pH 7.9). SAV0324 was loaded onto the column and the column was flowed with wash buffer (20mM Tris, 500mM NaCl, 10mM imidazole, pH 7.9) to remove any residual impurities before actual elutions were obtained. Using A buffer and B buffer (20mM Tris, 500mM NaCl, 500mM imidazole, pH 7.9), target protein was eluted against imidazole concentration gradient. SDS-PAGE was performed using samples before loading onto the column and elutions obtained from hexa-histidine tag purification. Initially purified proteins underwent buffer change into 20mM MES, 100mM NaCl, 1mM EDTA, 1mM BME, 0.1mM PMSF, pH 6.0 using 3K dialysis membrane and 1L of freshly made buffer. The buffer changed samples were concentrated in preparation for further purification by size-exclusion chromatography.

Same process was conducted for SAV0327 protein, except the final buffer ended up to be : 50mM Tris, 50mM NaCl, pH 8.0.

2.2.5 Size-Exclusion Chromatography (SEC)

Size exclusion chromatography (SEC) is a method to separate particles according to their size in solution. Therefore, size exclusion chromatography enables further purification of target protein from

other undesirable proteins or impurities (Paul-Dauphin, Morgan, and Herod, 2007).

The concentrated SAV0324 protein after dialysis and concentration were injected into HiLoad 16/600 Superdex 200pg and higher purity protein sample was obtained. SDS-PAGE was performed and the obtained fraction underwent further concentration in preparation for crystallization. The buffer used during size exclusion chromatography was freshly made, filtered, and degassed prior to sample injection.

Same process was conducted for SAV0327 protein.

2.2.6 Dialysis and Concentration

Dialysis is the process of separating molecules in solution through a semipermeable membrane, commonly used for buffer exchange (Reed, 2007).

After initial purification of SAV0324 through affinity chromatography, His-tag elution was inserted into the dialysis membrane. Snakeskin Dialysis Tubing 3.5K MWCO from Thermo Fisher Scientific was used in the process. The membrane was further dropped into 1L of 20mM MES, 100mM NaCl, 1mM EDTA, 1mM BME, 0.1mM PMSF, pH 6.0 buffer and was stored at 4°C overnight. The next day, protein after buffer exchange was removed from dialysis membrane and was concentrated using 10K Centrifugal Filters from Merck Millipore. The protein was concentrated to 1mM and was ready for crystallization.

Same process was conducted for SAV0327 protein except the buffer condition was 1L of 50mM Tris, 50mM NaCl, pH 8.0.

2.2.7 MALDI-TOF

MALDI-TOF (Matrix-Assisted Laser Desorption/Ionization Time-of-Flight) has many diverse applications. In proteomics, it is often used for identification of proteins (Karas and Hillenkamp, 1988).

Pure SAV0324 protein fraction obtained from his-tag purification was used to check the mass of the obtained sample. Comparing obtained mass and molecule weight of target protein, identification of protein is possible. MALDI-TOF measurements were made using Voyager-DE from Applied Biosystems.

2.2.8 Circular Dichroism (CD)

Circular Dichroism (CD) involves circularly polarized light and is observed when optically active material absorbs left- and right-handed light. CD spectroscopy can be applied in many different fields. Specifically in proteomics, the secondary structures of proteins can be predicted by far-UV (122-200nm) spectrums, tertiary structural information can be observed in near-UV (300-400nm) spectrum, and protein-metal interactions can be measured through visible CD spectroscopy (Whitmore and Wallace, 2008).

For secondary structure prediction, SAV0324 protein after buffer exchange into 20mM MES, 100mM NaCl, 1mM EDTA, 1mM BME, 0.1mM PMSF, pH 6.0 was used. Salt titration by CD spectroscopy was performed and Chirascan plus from Applied Photophysics was used for the process.

2.2.9 Crystallization

Protein crystallization occurs when the solution becomes supersaturated and the individual protein molecules pack in a repeating pattern (Rhodes, 2006).

Using concentrated (1mM) SAV0324 samples, crystal screening was performed using kits from Hampton Research at 20°C. Sitting-drop vapor-diffusion method was used. All reservoirs had 100 μL of crystallization reagent and each sitting drop was prepared by mixing 1μL of protein with 1μL of crystallization reagent.

Same process was conducted for SAV0327 protein but in addition to 20°C, 4°C incubation was also attempted.

2.2.10 Structure Determination

The crystals were soaked in 20% (v/v) glycerol and X-ray data was collected at PAL (Pohang, South Korea) using an ADSC quantum 315r CCD detector on 5C-SBII beamline at 100K. The raw data were processed using HKL2000 program.

Although good resolution data was obtained, no space group could be confirmed due to its twinning problem. Twinning occurs when two separate crystals share some of the same crystal lattice points in a symmetrical manner (Steinmetz et al., 2013). The presence of twinning was once again confirmed by Phenix (xtriage) and higher resolution data was collected again and the structure was solved using CCP4 program.

IV. Results

3.1 Polymerase Chain Reaction (PCR)

For amplification of SAV0324 protein, forward and reverse primers were designed (Table 1). The underlined sequences represent NdeI (CATATG) and XhoI (CTCGAG) enzyme restriction sites.

	Primer Sequence (5' → 3')
Forward Primer	CATATGAAAAAGTTAGCCAATTATTTATGG
Reverse Primer	CTCGAGAGCCTCCGGTAATGCTAG

Table 1. Primer sequence for SAV0324 PCR

Gradient PCR was performed using Bio-Rad T100 Thermal Cycler. The reaction mixture contained *S. aureus* genomic DNA, forward primer, reverse primer, and filtered distilled water. Temperature gradient was set from 50-65°C.

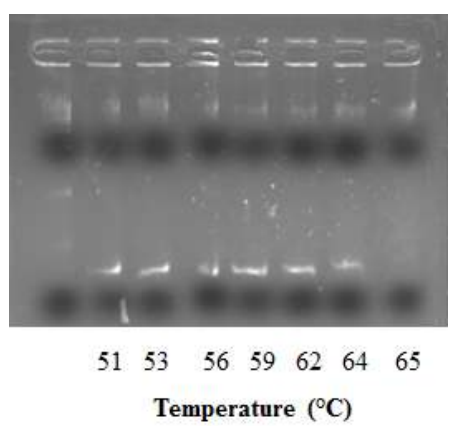

Figure 5. Gradient PCR of SAV0324

As a result, SAV0324 DNA was observed (Figure 5). DNA band was observed from 51-64°C and these fractions were collected and were PCR purified to remove everything except SAV0324 insert. The insert and pET21a(+) vector were treated with NdeI and XhoI restriction enzymes at 37°C for 3 hours and were purified again to remove residual enzymes and other contaminants. Then, resulting insert and vector were ligated together at 20°C for 1 hour and were further transformed with DH5α competent cell. Sequencing was performed at NICEM and as a result, SAV0324 was successfully cloned into pET21a(+) vector.

3.2 Overexpression and Solubility

SAV0324-pET21(+) plasmid was further transformed into 6 different competent cells : BL21DE3, BL21DE3Codon+, RosettaDE3, Rosetta2pLysS, C41DE3, and C43DE3. All 6 cells containing the plasmid were cultured in Luria-Bertani (LB) broth to determine which competent cells yielded the best overexpression of SAV0324 protein. The cells were grown until O.D. reached 0.5 and the resulting cultures were cooled at 4°C for 15 minutes. IPTG induction (0.25mM) was performed and the resulting cultures were incubated at 15°C for 20 hours. Samples were taken before IPTG induction (I-) and after 20 hours of incubation at 15°C (I+). Overexpression was observed at around 25 kDa after IPTG induction (Figure 6). C41DE3 and C43DE3 competent cells showed no overexpression, therefore only BL21DE3, BL21DE3Codon+, RosettaDE3, Rosetta2pLysS were further tested for protein solubility.

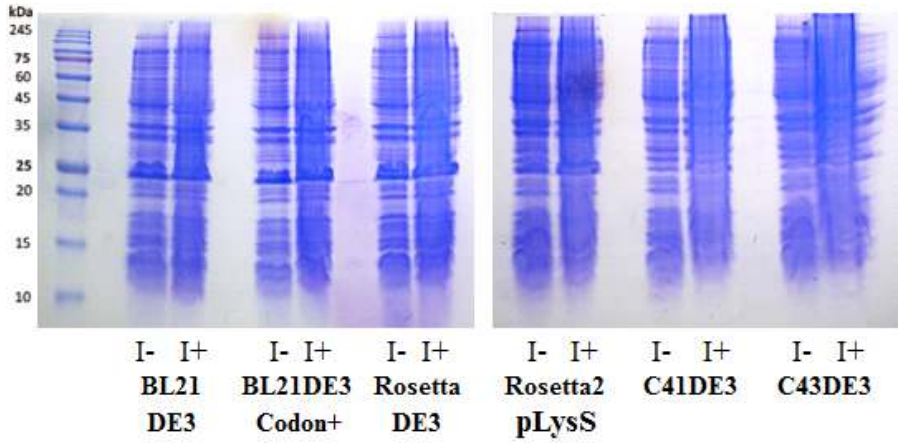

Figure 6. Overexpression of SAV0324 at 15°C.
SAV0324 protein is observed around 25 kDa.

All 6 cells were harvested and the resulting pellets were solubilized in 20mM Tris, 500mM NaCl, pH 7.9 along with 10% glycerol. Sample was taken before sonication (BS). The cells were suspended in a cold steel cup surrounded by crushed ice. The cells were sonicated using Cole-Parmer Ultrasonic Processor and sample was taken after sonication. The sample was centrifuged at 13,000rpm for 5 minutes and pellet (P) and supernatant (S) portions were separated. The samples were boiled at 95-100°C for around 10 minutes. SDS-PAGE was performed and solubility of protein was observed after cell lysis by sonication process (Figure 7). About half of the protein fell into inclusion bodies and half of the protein fell into its soluble fraction. Solubility of the protein enhanced significantly in low termperature incubation. The remaining lysate was centrifuged at 18,000rpm for 60 minutes at 4°C and the resulting supernatant was further filtered using 0.45μM filter in preparation for protein purification using immobilized metal affinity chromatography.

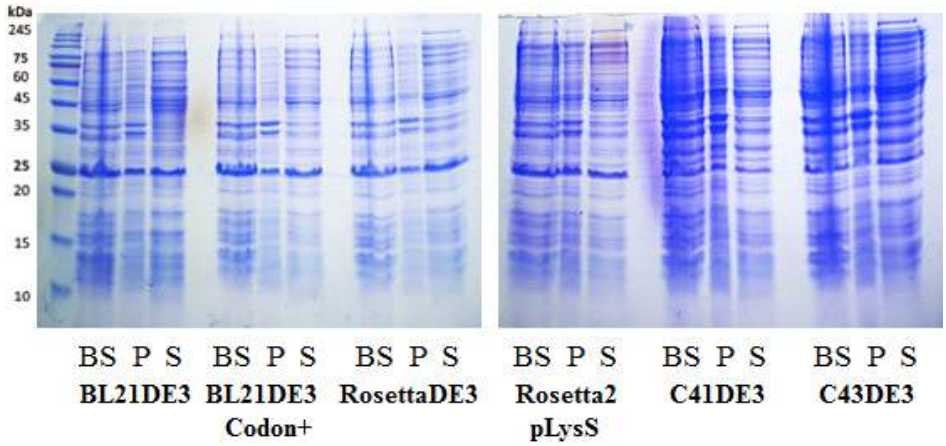

Figure 7. Solubility of SAV0324 at 15°C.
SAV0324 protein is observed around 25 kDa.

3.3 Purification (IMAC)

After soluble protein fraction was obtained, purification using hexa-histidine tag attached to C-terminus of SAV0324 protein was planned. Histidine tag has strong affinity to nickel and the protein would bind to the column and would elute upon applying imidazole gradient. IMAC using HiTrap Chelating HP column was washed in prior to protein loading in the following order: 0.1M EDTA, filtered distilled water, nickel ions, and A buffer (20mM Tris, 500mM NaCl, pH 7.9). The column was equilibrated with A buffer and the protein was loaded onto the column. After protein loading, two buffers were used : A buffer (20mM Tris, 500mM NaCl, pH 7.9) and B buffer (20mM Tris, 500mM NaCl, 500mM imidazole, pH 7.9). Imidazole gradient was applied to elute SAV0324 protein. The purified protein was confirmed by SDS-PAGE (Figure 8).

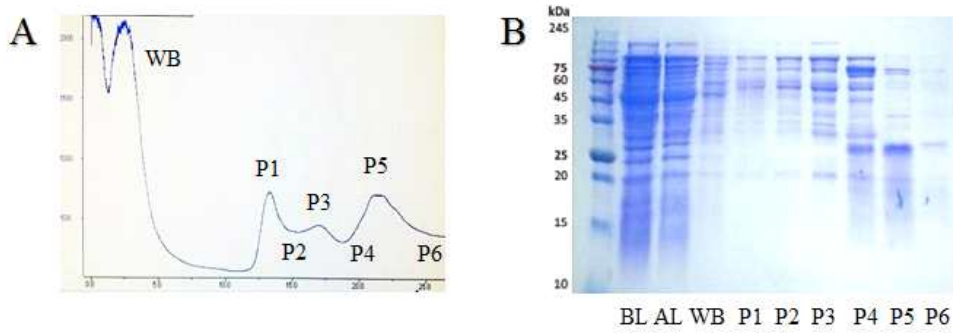

Figure 8. SAV0324 purification by IMAC.
(A) Peak profiles in FPLC. (B) SDS-PAGE. P5 represents SAV0324.

3.4 MALDI-TOF

In order to confirm the presence of SAV0324 protein, MALDI-TOF was used to measure the molecular weight distributions of the obtained his-tag elution.

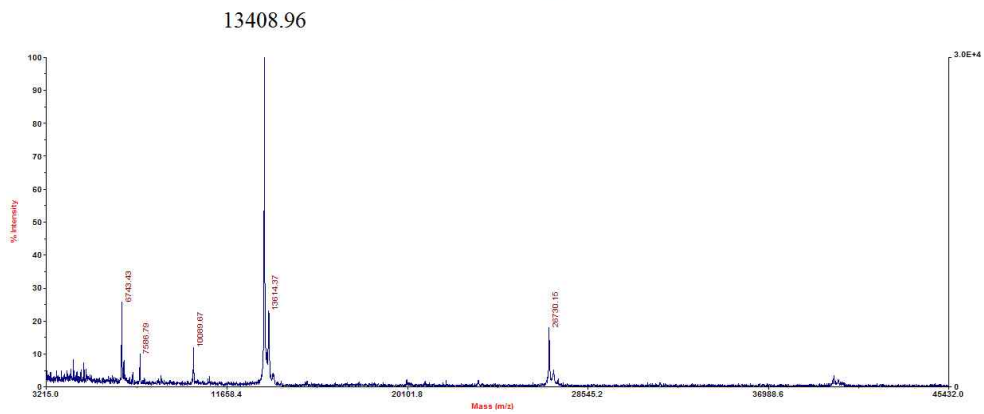

Figure 9. MALDI-TOF analysis of SAV0324 elution.
SAV0324 is represented by peak around 13.4 kDa.

After MALDI-TOF analysis, high peak was observed at 13408 Daltons. SAV0324 molecular weight is 13487 Daltons, therefore, the analysis confirmed the presence of SAV0324 protein within the obtained his-tag elution (Figure 9).

3.5 Circular Dichroism (CD)

After confirming the presence of SAV0324 protein, CD spectroscopy was conducted to predict the secondary structure of SAV0324. Buffer was exchanged from 20mM Tris, 500mM NaCl, pH 7.9 to 20mM MES, 100mM NaCl, 1mM EDTA, 1mM BME, 0.1mM PMSF, pH 6.0. The peak pattern showed between wavelength ranges 210-240nm revealed the protein conserved α-helices and β-strands in its structure in the new buffer condition (Figure 10).

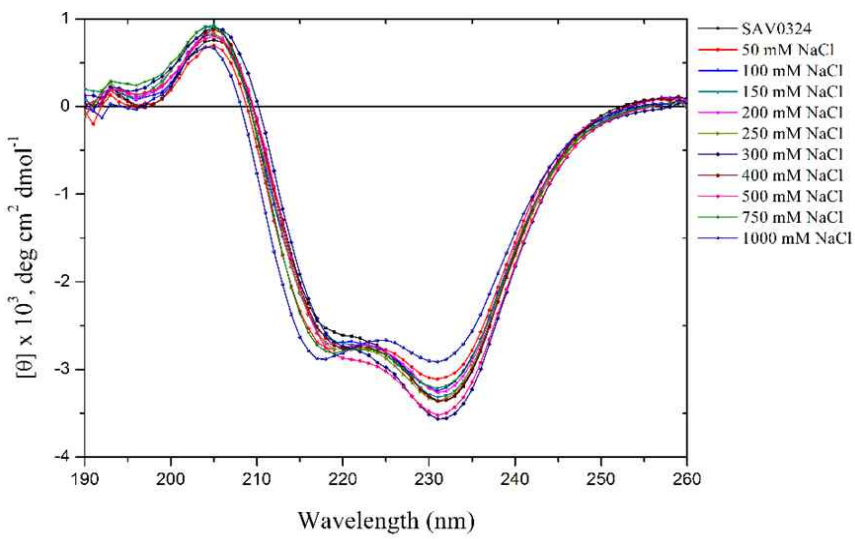

Figure 10. CD spectroscopy of SAV0324 after buffer exchange

3.6 Purification (SEC)

After buffer exchange was established (20mM MES, 100mM NaCl, 1mM EDTA, 1mM BME, 0.1mM PMSF, pH 6.0), the protein was concentrated down to 2mL in preparation for further purification. In size-exclusion chromatography, heavier molecules elute first and lightest molecules elute last. Thus, size-exclusion chromatography was conducted to remove further impurities obtained from IMAC. The concentrated protein was injected into HiLoad 16/600 Superdex 200pg column and the protein was eluted using the same buffer used during buffer exchange.

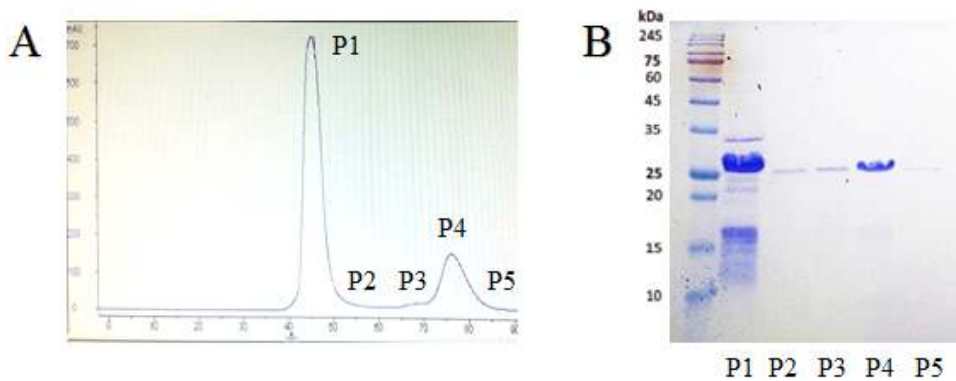

Figure 11. SAV0324 purification by SEC.
(A) Peak profiles in FPLC. (B) SDS-PAGE. P1 represents SAV0324.

SDS-PAGE showed SAV0324 protein in all peaks obtained from size exclusion chromatography (Figure 11). Although P4 seemed more pure compared to P1, P1 showed the greatest UV intensity. P1 showed several other bands, however P1 was chosen to attempt protein crystallization.

3.7 Crystallization

The elution (P1) obtained from size-exclusion chromatography was concentrated down to 1mM in preparation for crystallization. Protein precipitation was observed during concentration and were removed regularly to avoid further precipitation of protein. Six different crystallization kits from Hampton Research and Molecular Dimensions were used (Structure Screen 1 & 2, Crystal Screen Lite, Index, PEG/ION & PEG2/ION, and Wizard 1, 2, 3, and 4). Crystallization was performed using sitting-drop vapor diffusion method at 20°C. The reservoir contained 100μL volume and the droplets were setup carefully to avoid formation of air bubbles. After 2-3 days after crystal setup, crystals were formed from PEG2/ION #10 solution (Figure 12).

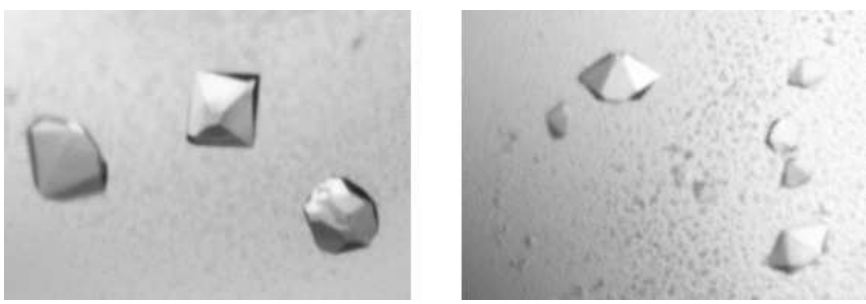

Figure 12. SAV0324 protein crystals

The crystallization reagent component was 8% Tacsimate pH 4.0, 20% w/v PEG3350 and was not coated with cryoprotectant solution. These crystals were shown to be best at diffraction compared to other conditions (Figure 13) and the protein crystal diffracted at 1.88Å.

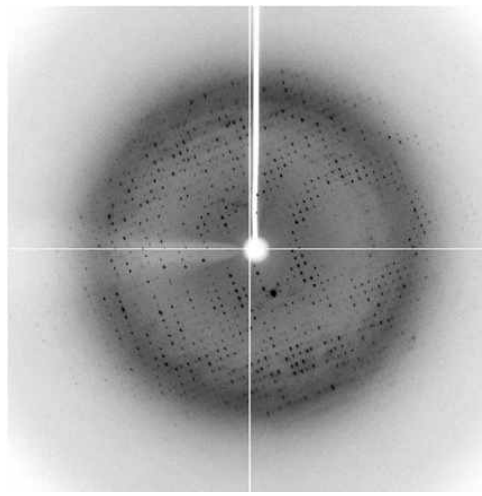

Figure 13. SAV0324 crystal diffraction pattern

3.8 Structure Determination

3.8.1 SAV0324 Structure

Although the protein crystal showed great diffraction, no space group was confirmed. Upon zooming in to the diffraction pattern, twinning problem was observed. Presence of twinning was confirmed by Phenix (xtriage) and higher resolution of protein crystal was collected again and the structure of the SAV0324 protein was solved using CCP4 program (using twinning).

SAV0324 protein existed in its monomeric form and conserved five α-helices and nine β-strands in its structure. The nine β-strands ran antiparallel to each other and were more dominant compared to its α-helical components (Figure 14).

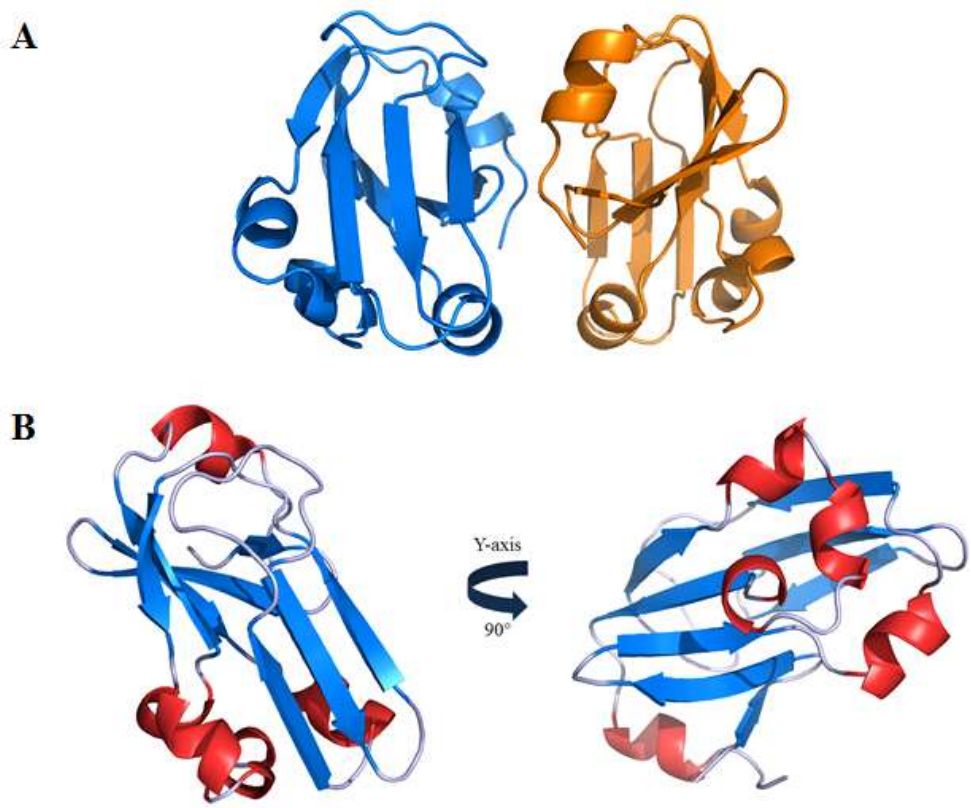

Figure 14. Protein structure of SAV0324. (A) Two monomers aligned in an asymmetric unit. (B) Single SAV0324 protein.

The crystal belonged to the hexagonal space group $P6_5$, with unit cell parameters of a = 85.40 Å, b = 85.40 Å, c = 68.35 Å and α = 90°, β = 90°, γ = 120°C. Raw data were processed and scaled using HKL 2000 program package. After structure calculation, the results showed that the two monomers of SAV0324 protein were aligned in an asymmetric unit (Figure 14A). Although the structure seemed like a homo-dimer, the protein's monomeric state was confirmed by MALDI-TOF analysis and gel filtration chromatography.

3.8.2 Crystal Data Collection & Refinement

The crystals were maintained around near 20°C at all times. The data was collected at PAL using an ADSC quantum 315r CCD detector on 5C-SBII beamline at 100K and the resolution turned out to be 1.88 angstroms. After calculation of the protein structure, refinement statistics were obtained (Table 2). The obtained data showed great protein crystal diffraction and the values of R-work and R-free values were also kept in the low and excellent range. Stated previously, the crystal belonged to the hexagonal space group $P6_5$, with unit cell parameters of a = 85.40 Å, b = 85.40 Å, c = 68.35 Å and α = 90°,β = 90°, ɣ = 120°C and the completeness of the data was also very satisfactory.

Wavelength	0.9795
Resolution range	25.87 - 1.88 (1.91 - 1.88)
Space group	P 65
Unit cell	85.40 85.40 68.35 90 90 120
Unique reflections	22991 (1158)
Completeness (%)	99.4 (100.0)
Mean I/sigma(I)	75.67 (15.51)
Wilson B-factor	30.5
Average B-factor	35.0

R-work	17.53
R-free	18.95
RMS(bonds)	0.011
RMS(angles)	1.572
Ramachandran	
favored (%)	98.61[a]
allowed (%)	1.39[a]
outliers (%)	0.00[a]
Clashscore	5.19[a] (96th percentile)

Table 2. Crystal data collection and refinement

3.8.3 Ramachandran Plot

A Ramachandran plot is often used to visualize backbone dihedral angles psi (ψ) against phi (ϕ) of amino acid residues in protein structures. In other words, the plot is often used to show the empirical distribution of data points in a protein structure. The inner light-blue boundary corresponds to the core and favored regions which represents the most favorable combinations of psi and phi values. The outer dark-blue boundary corresponds to the allowed regions of psi and phi values.

As the results shown below, 100% of the data points lay in allowed regions and 98.6% of the data points lay in favored regions (Figure 15). Since majority of data points lay in core and favored regions, the streochemical quality of the obtained data was satisfactory. Lastly, there were no outliers in the obtained data and thus the model of the calculated SAV0324 protein structure was predicted to be favorable.

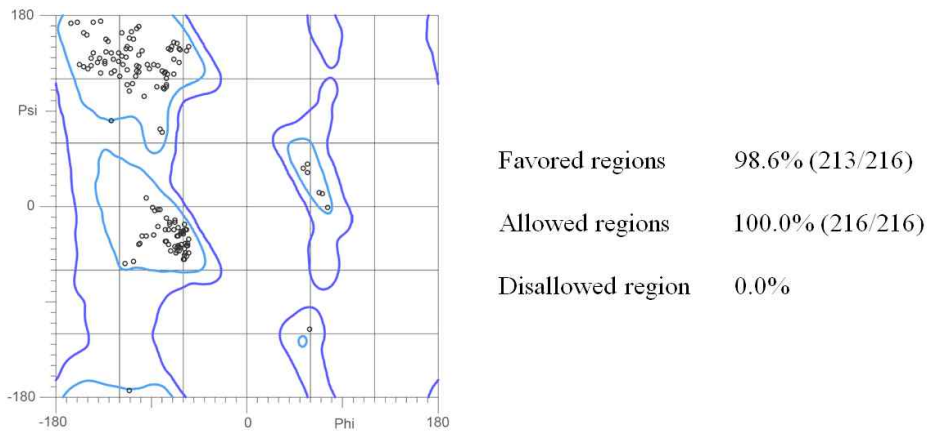

Figure 15. Ramachandran plot of SAV0324

3.8.4 Topology

The two-dimensional representation of SAV0324 protein structure was also calculated using PDBSum server and ProOrigami Server (Figure 16). The figures clearly showed five alpha helices and nine beta strands which ran antiparallel with one another. Specifically starting from the N-terminus, beta strands #1-3 ran antiparallel with one another, beta strands #4-6 ran antiparallel with one another and beta strands #7-9 ran antiparallel with one another.

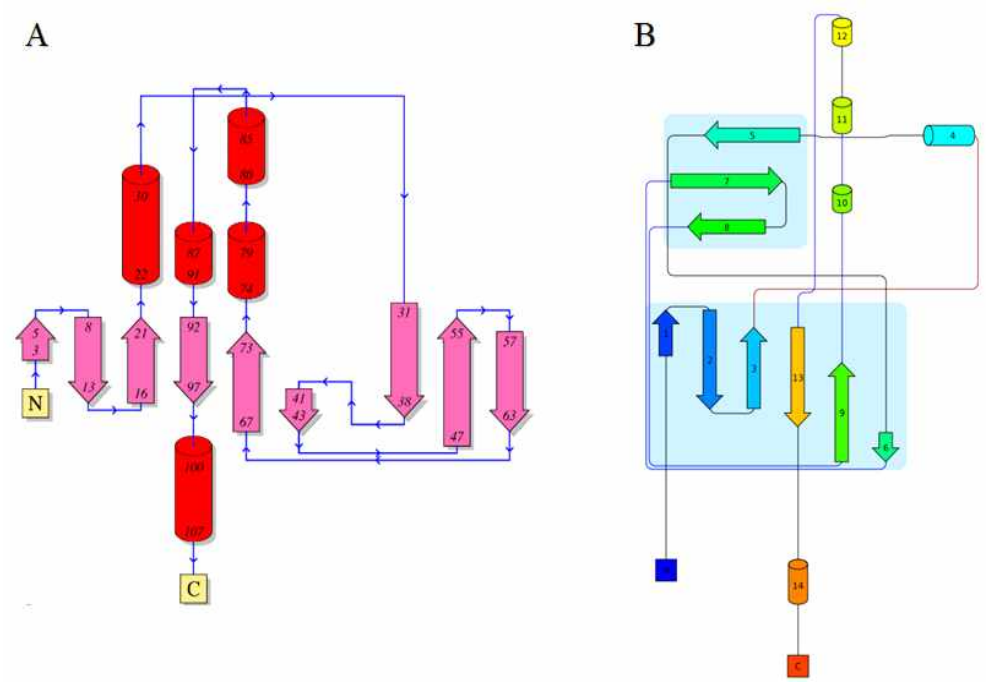

Figure 16. Topology of SAV0324. Calculated using: (A) PDBSum server (B) ProOrigami Server

3.8.5 Homology Search

After structure determination of SAV0324 protein, SAV0324's homologue structures were searched using DALI server. Among several homologues, three homologues with highest structural similarities were chosen for comparison (Figure 4). Protein PDB ID : 5A35 had 60% sequence similarity and same function with that of SAV0324 protein. The other proteins had lower sequence identity, but shared same or similar function with that of SAV0324 protein.

No.	PDB ID	Residues	Sequence Identity	Function
1	5A35	112	60%	Glycine Cleavage H Protein
2	3AB9	127	25%	Glycine Cleavage H Protein
3	3A8I	128	25%	Aminomethyltransferase
4	3A8K	126	25%	Aminomethyltransferase

Table 3. Homologues of SAV0324 protein and characteristics.

Aside from sequence similarity, the degree of structural similarities were represented by z-scores (Figure 17A). Specifically, one homologue (PDB ID: 5A35) had z-score of 22.1, which can be interpreted as remarkable structural similarity between SAV0324 and 5A35 protein. Also, 5A35 and 3AB9 and proteins showed very high structural similarity with SAV0324 protein with z-scores of 16.3. Normally, z-scores higher than 3.0 represent data in 99^{th} percentile. Therefore, z-score of 22.1 and 16.3 show the remarkable similarity between SAV0324 and its homolouges. The structural similarity was also observed through superimposition of SAV0324 protein with 5A35, 3AB9, and 3A8I proteins (Figure 17B).

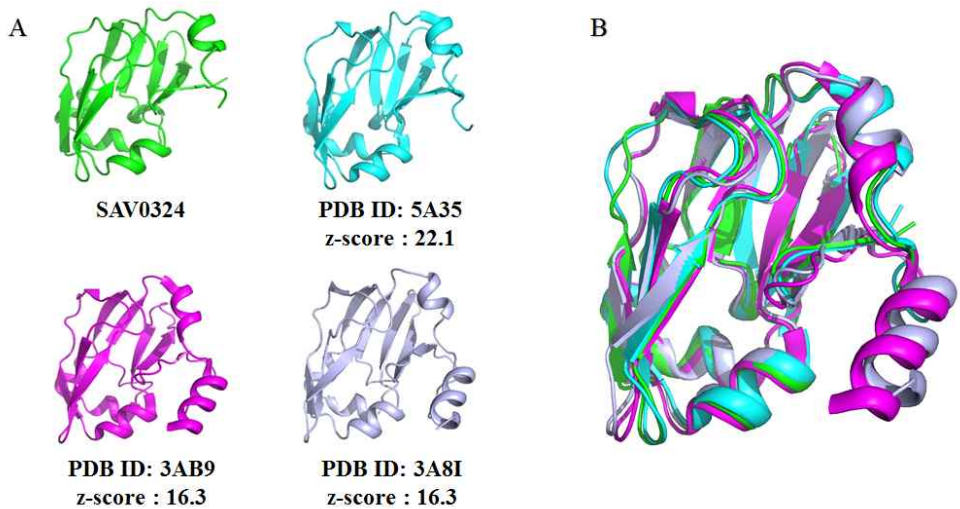

Figure 17. SAV0324 homology search. (A) SAV0324's homologues (B) Superimposition of SAV0324 and its homologues

Protein's structure is known to determine its function. Therefore, structural similarity between SAV0324 and its homologues may lead to similar functions between these proteins. Surprisingly, 5A35 and 3AB9 proteins were also shown to have glycine cleavage system H-like protein (GcvH-L) functionality. The other two homologues, 3A8I and 3A8K proteins, had different functionality. However, they shared the similarity in the aspect that glycine cleavage system H-like protein acts as a carrier for lipoyl moiety while aminomethyltransferase acts as a carrier for amino methyl groups. Future comparison of protein structures and active sites between SAV0324 and its homologues might reveal key residues responsible affecting their function and thus may reveal key clues to understanding lipoylation.

3.9 Active Site

The active sites of SAV0324 protein was determined by other researchers prior to structure determination (Figure 18). They showed that mutations of lipoylation motif residues within SAV0324 impair the lipoate transfer reaction. Mutation of K56 (56th lysine) residue interfered with lipoyl attachment, whereas E53 (53rd glutamate) residue was important for recognition by SAV0327. Specifically, mutation of E53 residue significantly decreased lipoylation and mutation of K56 resulted in no lipoylation at all (Rack et al., 2015).

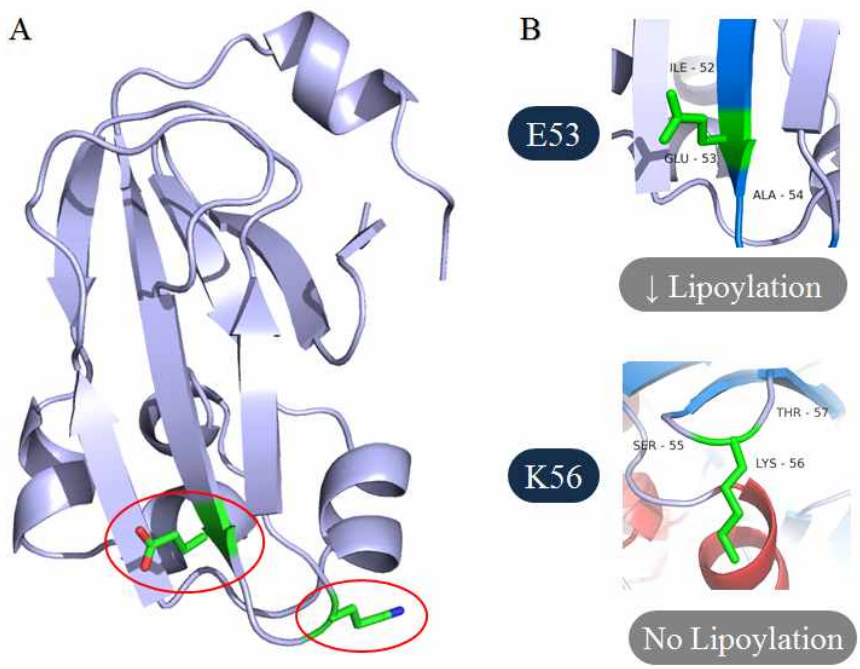

Figure 18. Active sites of SAV0324 protein
(A) Active sites indicated by red circle
(B) Two residues involved in lipoylation

3.10 Binding Test

The direct binding between SAV0324 and SAV0327 proteins were tested in order to see if the proteins had any protein-to-protein interaction. Binding test was conducted both in the presence and absence of lipoic acid. In the presence of lipoic acid, precipitation in both proteins were observed and further experiment couldn't be conducted. In the absence of lipoic acid, all of SAV0327 protein flowed out in the loading pass and only SAV0324 protein was eluted against imidazole gradient (Figure 19). If the proteins had any binding interaction, both proteins would elute against imidazole gradient, not only one protein by itself since only SAV0324 protein had hexahistidine tag attached to its C-terminus. Therefore, there are no direct binding between SAV0324 and SAV0327 proteins in the absence of lipoic acid.

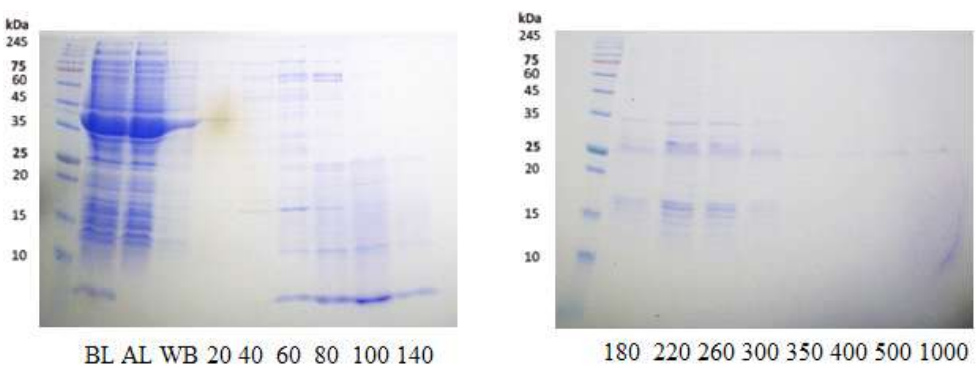

Figure 19. Binding test between SAV0324 and SAV0327.
All of SAV0327 flowed out in loading pass (AL) and wash buffer (WB) around 35 kDa. Only SAV0324 was eluted against imidazole gradient, observed around 25 kDa between 220 - 300 mM imidazole.

3.11 SAV0327

3.11.1 Cloning, Overexpression, and Solubility

For amplification of SAV0327 protein, forward and reverse primers were designed (Table 4). The underlined sequences represent NdeI (CATATG) and XhoI (CTCGAG) enzyme restriction sites.

	Primer Sequence (5' → 3')
Forward Primer	GGGAATTCCATATGTACTTAATAGAACCG
Reverse Primer	CCGCTCGAGACTTAAAATCATCTCAACC

Table 4. Primer sequence for SAV0327 PCR

Gradient PCR was performed using Bio-Rad T100 Thermal Cycler. The reaction mixture contained *S. aureus* genomic DNA, forward primer, reverse primer, and filtered distilled water. Temperature gradient was set from 50-65°C.

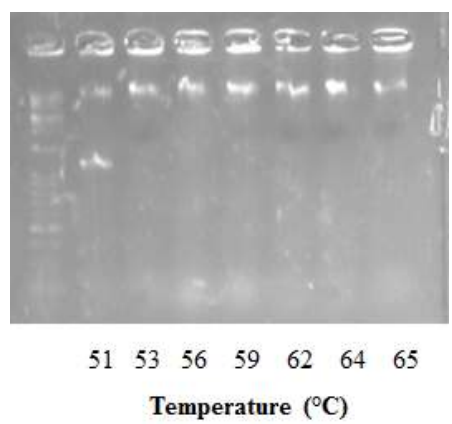

Figure 20. Gradient PCR of SAV0327
The protein is cleared observed between 53-64°C.

As a result, SAV0327 DNA was observed (Figure 20). DNA band was observed from 53-64°C and these fractions were collected and were PCR purified to remove everything except SAV0327 insert. The insert and pET21a(+) vector were, treated with NdeI and XhoI restriction enzymes at 37°C for 3 hours and were purified again to remove residual enzymes and other contaminants. Then, resulting insert and vector were ligated together at 20°C for 1 hour and were further transformed with DH5α competent cell. Sequencing was performed at NICEM and as a result, SAV0327 was successfully cloned into pET21a(+) vector.

SAV0327-pET21(+) plasmid was further transformed into 6 different competent cells : BL21DE3, BL21DE3Codon+, RosettaDE3, Rosetta2pLysS, C41DE3, and C43DE3. All 6 cells containing the plasmid were cultured in Luria-Bertani (LB) broth to determine which competent cells yield the best overexpression of SAV0327 protein. The cells were grown until O.D. reached 0.5 and the resulting cultures incubated at two different temperatures to determine which temperature yield the best protein overexpression and solubility. One temperature was IPTG induction at 0.5mM and incubation at 37°C - 180rpm for 4 hours and the other temperature was IPTG induction at 0.25mM and incubation at 15°C for 20 hours. The low temperature incubation were cooled at 4°C for 15 minutes prior to IPTG induction. Samples were taken before IPTG induction (I-) and after IPTG induction and further 4 hours of incubation at 37°C and 20 hours of incubation at 15°C were performed separately (I+). Overexpression was observed after IPTG induction (Figure 21). SAV0327-pET21a-BL21DE3 was chosen for further solubility test.

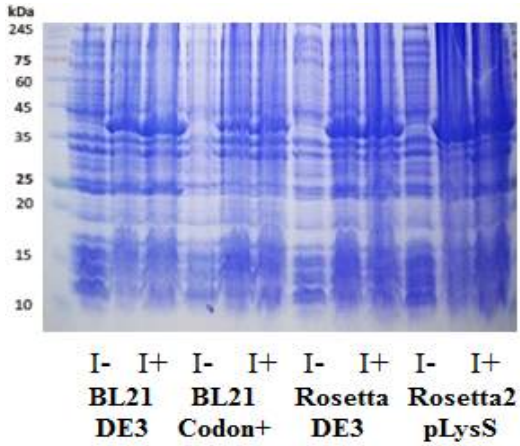

Figure 21. Overexpression of SAV0327 at 37°C & 15°C
The protein is clearly observed around 37 kDa.

All 6 cells were harvested and the resulting pellets were solubilized in 20mM Tris, 500mM NaCl, pH 7.9 along with 10% glycerol. Sample was taken before sonication (BS). The cells were suspended in a cold steel cup surrounded by crushed ice. The cells were sonicated using Cole-Parmer Ultrasonic Processor and sample was taken after sonication. The sample was centrifuged at 13,000rpm for 5 minutes and pellet (P) and supernatant (S) portions were separated. The samples were boiled at 95-100°C for 10 minutes. SDS-PAGE was performed and solubility was observed after cell lysis by sonication process (Figure 22). At 37°C about half of the protein fell into inclusion bodies and about half of the protein fell into soluble fraction. However at 15°C, about 10% of the protein fell into inclusion bodies and about 90% of the protein fell into soluble fraction. Solubility of the protein enhanced significantly in low temperature incubation. SAV0327-pET21a(+)-BL21DE3 at 15°C culture was chosen for further purification using immobilized metal affinity chromatography.

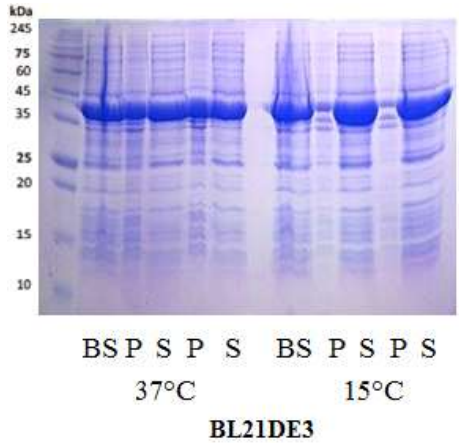

Figure 22. Solubility of SAV0327 at 37°C & 15°C
High solubility is observed at 15°C.

3.11.2 Purification (IMAC and SEC)

After soluble protein fraction was obtained, purification using hexa-histidine tag attached to C-terminus of SAV0324 protein was planned. Histidine tag has strong affinity to nickel and the protein would bind to the column and would elute upon applying imidazole gradient. IMAC using HiTrap Chelating HP column was washed in prior to protein loading in the following order: 0.1M EDTA, filtered distilled water, nickel ions, and A buffer (20mM Tris, 500mM NaCl, pH 7.9). The column was equilibrated with A buffer and the protein was loaded onto the column. After protein loading, two buffers were used : A buffer (20mM Tris, 500mM NaCl, pH 7.9) and B buffer (20mM Tris, 500mM NaCl, 500mM imidazole, pH 7.9). Imidazole gradient was used to obtain SAV0327 protein. The purified protein was confirmed by SDS-PAGE (Figure 22).

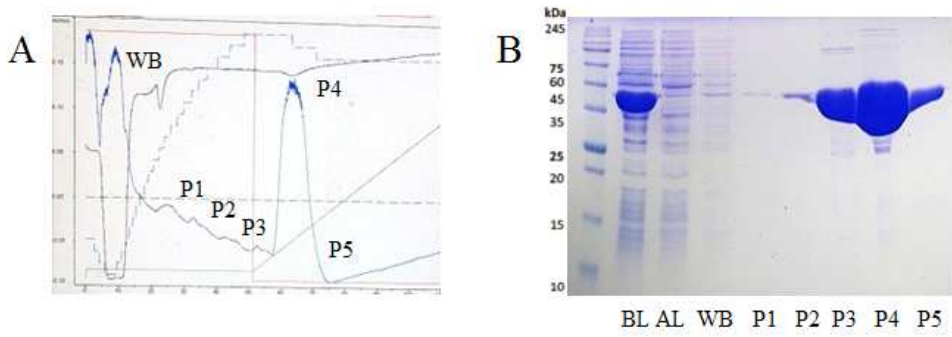

Figure 23. SAV0327 purification by IMAC
(A) Peak profiles in FPLC. (B) SDS-PAGE. P4 represents SAV0327

After buffer exchange was established (50mM Tris, 50mM NaCl, pH 8.0), the protein was concentrated down to 2mL in preparation for further purification. In size-exclusion chromatography, heavier molecules elute first and lightest molecules elute last. Thus, size-exclusion chromatography was conducted to remove further impurities obtained from IMAC. The concentrated protein was injected into HiLoad 16/600 Superdex 200pg column and the protein was eluted using the same buffer used during the buffer exchange.

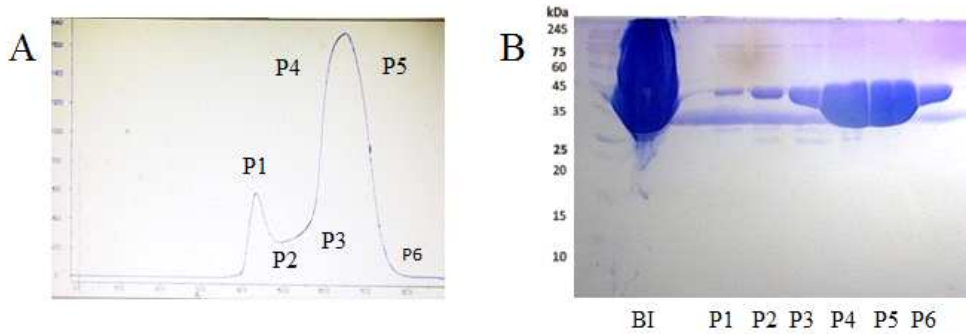

Figure 24. SAV0327 purification by SEC
(A) Peak profiles in FPLC
(B) SDS-PAGE. P4 and P5 represents SAV0324

SDS-PAGE showed SAV0327 protein in all peaks obtained from size-exclusion chromatography (Figure 24). P4 and P5 showed the greatest UV intensity and these two fractions were collected together to attempt protein crystallization.

3.11.3 Crystallization

The elutions (P4 and P5) obtained from size-exclusion chromatography was concentrated down to 1mM in preparation for crystallization. Six different crystallization kits from Hampton Research and Molecular Dimensions were used (Structure Screen 1, Structure Screen 2, Crystal Screen Lite, Index, PEG/ION, PEG2/ION, Wizard 1, Wizard 2, Wizard 3, and Wizard 4). Crystallization was performed using sitting-drop vapor diffusion method at 20°C and 4°C. The reservoir contained 100μL volume and the droplets were setup carefully to avoid formation of air bubbles. As a result, many crystals were formed after as short as one day to as long as two weeks (Figure 25).

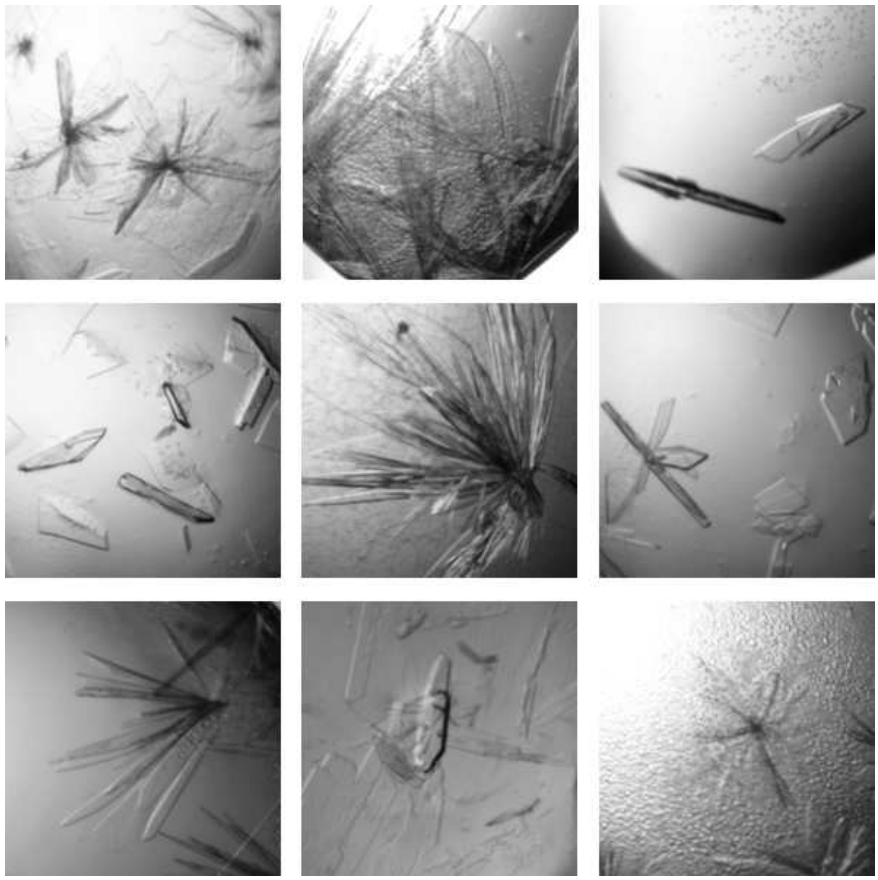

Figure 25. SAV0327 protein crystals

V. Discussion

The process of lipoylation is crucial in understanding and controlling bacterial virulence of S*taphylococcus aureus*. SAV0324 protein acts as a carrier for lipoyl moiety and undergoes lipoylation by SAV0327 protein. The protein further undergoes ADP-ribosylation only if SAV0324 is in its lipoylated form. Since ADP-ribosylation cycle is known to modulate virulence of the bacteria, inhibition at the lipoylation step would be important in decreasing bacterial virulence.

In this study, SAV0324 protein was successfully cloned into pET21a(+) vector. The protein was overexpressed in BL21DE3Codon+ cells and soluble fraction was observed after 20 hours of 15°C incubation. The protein was then initially purified using immobilized metal affinity chromatography (IMAC) and was further purified using size exclusion chromatography (SEC). The protein's presence was confirmed by MALDI-TOF analysis through comparing its peak with SAV0324's molecular weight. Buffer exchange was performed into 20mM MES, 100mM NaCl, 1mM EDTA, 1mM BME, 0.1mM PMSF, pH 6.0 using dialysis membrane. CD spectroscopy was performed and the protein was shown to conserve its secondary structure throughout various salt concentrations. The protein was concentrated down to 1mM and was crystallized at 20°C using kits from Hampton Research and Molecular Dimensions. The crystals were sent to PAL for X-ray diffraction data collection, using an ADSC quantum 315r CCD detector on 5C-SBII bealimline at 100K. The raw data were processed using HKL2000 program and the structure of SAV0324 was solved by molecular replacement method using CCP4 program.

SAV0324 protein's structure was determined and there were five alpha helices and nine beta strands conserved in its structure. Through further experiments by Rack in 2015, the two lipoylation sites in SAV0324 were determined. They showed that mutation of E53 (53rd glutamate) resulted in significant decrease in lipoylation and mutation of K56 (56th lysine) resulted in no lipoylation at all.

Using DALI server, the structural homologues of SAV0324 protein were obtained. One homologue, 5A35 protein showed remarkable sequence identity (60%) and structural similarity (z-score = 22.1). Although not as much as 5A35, the other homologues showed very high structural similarity as well (z-score = 16.3). Superimposition of SAV0324 protein and all homologues showed overlap of the structures in vast majority of regions and showed remarkable sequence similarity. The homologues also shared same or similar functions to that of SAV0324 protein and therefore, by comparing the active sites of the homologues to SAV0324 protein, key clues to understanding lipoylation may be revealed.

In the binding test between SAV0324 and SAV0327 proteins, the experiment showed there was no direct binding between SAV0324 and SAV0327 proteins. However, one major fault in this experiment was that the experiment was conducted in the absence of lipoic acid. Theoretically, the proteins are known to interact together when lipoyl moiety is available; yet, the proteins showed heavy precipitation upon addition of lipoic acid *in vitro*. Therefore, the results of the binding test is not at all reliable as there was no lipoyl moiety available. However, the fact that the two proteins do not bind directly in the absence of lipoic acid is also important to note. The future experiments will be to optimize conditions to conduct the experiment again in the presence of lipoyl moiety.

In addition to SAV0324 protein's structure, SAV0327 protein structure determination process was initiated. The protein was successfully cloned into pET21a(+) vector and was overexpressed in BL21DE3 cells. Soluble fraction was obtained after 20 hours of incubation at 15°C and the protein was purified using immobilized metal affinity chromatography and size-exclusion chromatography. Buffer exchange was performed into 50mM MES, 50mM NaCl, pH 8.0 and the protein was concentrated down to 1mM. Crystallization attempts have been made using crystallization kits from Hampton Research and Molecular Dimensions at both 20°C and 4°C. Many crystal hits were obtained for X-ray beamline analysis.

Ultimately, the future and last plan is to proceed with drug candidate screening using SAV0324 protein's structural information and active sites as a template. The goal would be to determine compounds which are capable of inhibiting lipoylation of SAV0324 and further proceed with lead optimization. If any of the drug candidates successfully inhibits lipoylation of SAV0324, the molecule will ultimately reduce the bacteria's ability to cause a disease. Also, determination of SAV0327's structure and active sites will be focused to fully understand lipoylation process. Understanding the process thoroughly would be critical in understanding and controlling bacterial virulence of *Staphylococcus aureus*.

References

Masalha, M; et al. (2001). Analysis of Transcription of the Staphylococcus Aureus Aerobic Class Ib and Anaerobic Class III Ribonucleotide Reductase Genes in Response to Oxygen. *Journal of Bacteriology*. **183** (24): 7260 - 7272.

Chambers, H.F. and DeLeo, F.R. (2009). Waves of Resistance : *Staphyloccocus aureus* in the antibiotic era. *Nature Reviews : Microbiology*. **7** : 629 - 641.

Chambers, H.F. (2001). The Changing Epidemiology of *Staphylococcus aureus*? *Emerging Infectious Diseases*. **7** (2): 178 - 182.

Cheesbrough, M. Medical Laboratory Manual for Tropical Countries, Vol. 2: *Microbiology and AIDS Supplement*. Cambridgeshire, UK: Tropical Health Technology, 1991. Print.

Dinges, M.M., Orwin, P.M., Schlievert, P.M. (2000). Exotoxins of Staphylococcus aureus. *Clin. Microbiol. Rev.* **13** (1): 16 - 34

Bohn, C., Rigoulay, C., Chabelskaya, S., Sharma, C.M., Marchais, A., Skorski, P., Borezee-Durant, E., Barbet, R., and Jacquet, E. (2010). Experimental discovery of small RNAs in Staphylococcus aureus reveals a riboregulator of central metabolism. *Nucleic Acids Research*. **38** (19): 6620 - 6636.

Archer, G.L. (1998). *Staphylococcus aureus*: A Well-Armed Pathogen. *Clinical Infectious Diseases*. **26** : 1179 - 1181.

Weigel, L.M, Clewell, D.B., Gill, S.R., Clark, N.C., McDougal, L.K., Flannagan, S.E., Kolonay, J.F., Shetty, J., Killgore, G.E., and Tenover, F.C. (2003). Genetic Analysis of a High-Level Vancomycin-Resistant Isolate of *Staphylococcus aureus*. *Science*. **302** : 1569 - 1571.

Grundmann, H., Aires-de-Sousa, M., Boyce, J., and Tiemersma, E. (2006). Emergence and resurgence of methicillin-resistant *Staphylococcus aureus* as a public-health threat. *Lancet*. **368** : 874-885.

Rack, J.G.M., Morra, R., Barkauskaite, E., Leys, D., Traven, A., and Ahel, I. (2015). Identification of a Class of Protein ADP-Ribosylating Sirtuins in Microbial Pathogens. *Molecular Cell*. **59** : 309 - 320.

Deng, Q. and Barbieri, J.T. (2008). Molecular mechanisms of the cytotoxicity of ADP-ribosylating toxins. *Annual Review of Microbiology*. **62** : 271 - 288.

Saiki, R., Gelfand, D., Stoffel, S., Scharf, S., Higuchi, R., Horn, G., Mullis, K., and Erlich, H. (1988). Primer-directed enzymatic amplification of DNA with a thermostable DNA polymerase. *Science*. **239** (4839): 487 - 491.

Marbach A. and Bettenbrock, K. (2012). lac operon induction in Escherichia coli: Systematic comparison of IPTG and TMG induction and influence of the transacetylase LacA. *Journal of Biotechnology*. **157** (1): 82 - 8.

Ninfa, A.J., Ballou, D.P., and Benore, M. (2009). Fundamental Laboratory Approaches for Biochemistry and Biotechnology (2 ed.). Wiley. p. 133

Paul-Dauphin, S., Morgan, M., and Herod, K. (2007). Probing Size Exclusion Mechanisms of Complex Hydrocarbon Mixtures: The Effect of Altering Eluent Compositions. *Energy & Fuels*. **6**. 21 (6): 3484 - 3489.

Reed, R. (2007). Practical Skills in Biomolecular Sciences, 3rd ed. Essex: Pearson Education Limited. p. 379.

Karas, M. and Hillenkamp, F. (1988). Laser desorption ionization of proteins with molecular masses exceeding 10,000 daltons. *Analytical Chemistry*. **60** (20): 2299 - 301.

Whitmore, L. and Wallace, B.A. (2008). Protein secondary structure analyses from circular dichroism spectroscopy: methods and reference databases. *Biopolymers*. **89** (5): 392 - 400.

Rhodes, G. (2006) Crystallography Made Crystal Clear, Third Edition: A Guide for Users of Macromolecular Models, 3rd Ed., Academic Press

Steinmetz, D.R., Jäpel, T., Wietbrock, B., Eisenlohr, P., Gutierrez-Urrutia, I., Saeed (2013), Revealing the strain-hardening behavior of twinning-induced plasticity steels: Theory, simulations, experiments, 61, Acta Materialia, p. 494

국문초록

X-선 결정학에 의한 황색포도상구균 유래 SAV0324 단백질의 구조 연구

구 지 성

서울대학교 대학원

약학과 물리약학 전공

황색포도상구균은 그람양성 병원성 박테리아이다. 대략 20~30%의 인구가 보균자이며 강한 항생제 내성을 가질 수 있다. 또한, 인체에 해로운 독소와 작은 RNA들을 생성하며, 황색포도상구균은 인체 내에 수많은 질병을 일으키고 전 세계적으로 많은 질병과 사상자를 일으키는 원인이 된다.

SAV0324 단백질은 glycine cleavage system H-like protein (GcvH-L)이며 리포산 운반체 역할을 한다. SAV0327 단백질에 의하여 SAV0324단백질과 리포산과 결합하여 lipoylated가 되며 이 과정 없이는 ADP-리보실화가 진행되지 않는다. ADP-리보실화가 이루어지지 않으면 황색포도상구균 박테리아의 독성이 감소가 되며, 그러한 이유로 lipolyation을 제어하는 것이 매우 중요하다.

Structure Based Drug Design (SBDD)의 지식을 바탕으로 하여 X-선 결정학으로 SAV0324 단백질의 구조를 1.88 A의 해상도로 밝혀내었다. 황색포도상구균 SAV0324 단백질은 단량체였으며 5개의 alpha helix와 9개의 beta strand로 형성되어 있다. Lipoylation 활성 부위는 SAV0324 단백질의 56번째 라이신 잔기로 알려져 있으며 정확한 lipoylation의 과정을 밝히기 위하여 SAV0327 단백질의 결정화도 성공하였다. 두 단백질을 상호작용을 확인하기 위하여 결합 실험을 진행한 결과, 두 단백질은 직접 결합을 하지는 않았다. 밝혀진 SAV0324의 구조와 더불어 SAV0327의 구조와 활성 부위를 함께 밝혀낸다면 황색포도상구균의 병독성 억제에 대한 정보를 제공할 것이다.

주 요 어 : Structure Based Drug Design (SBDD),
***Staphylococcus aureus*, X-ray crystallography,**
SAV0324, lipoylation, inhibition

학 번 : 2015-23174